

Influence of Cutting Tool and Drilling Process on the Machinability of Inconel 718

L.J. Ma^{1*}, H. Yu², X.H. Mao³, C.R. Li⁴, C.Y. Feng⁵, F.N. Li⁶

School of Mechanical and Electrical Engineering, Henan Institute of Science and Technology, Xinxiang, 453003, China

*Email: mlj001@163.com

ORCID: ¹0000-0002-8632-8044, ²0000-0001-5811-6645, ³0000-0002-9076-958X, ⁴0000-0003-2961-4375, ⁵0000-0003-1233-9661, ⁶0000-0001-6634-5501

Nickel-based superalloy is a kind of metal material that is widely used to manufacture high-temperature parts in the fields of aviation and aerospace, but it is also a typical difficult-to-cutting material. The precision cutting of nickel-based superalloy has always been an important manufacturing problem. Based on the tests of conventional drilling with three kinds of twist drills, the machinability of Inconel 718 was evaluated comprehensively by drilling force, tool wear and machining quality, and the cutting tools suitable for drilling nickel-based superalloy were chosen. Then the experiments of peck-drilling for Inconel 718 were carried out, and the process effect under different peck depth Q was deeply researched. The results showed that the HSS-Co (high speed steel with cobalt) twist drill can meet the needs of low-speed drilling of nickel-based superalloy, while the coated carbide twist drill has better service performance. The drill tip structure of dual clearance angle is beneficial to decrease the cutting friction and improve the machining accuracy. Compared with conventional drilling, the peck-drilling can reduce the cutting force and improve the dimensional accuracy and surface quality. However, it is very important to choose a suitable peck depth Q for fully exploiting the advantages of peck-drilling.

Keywords: Nickel-based superalloy, machinability, cutting tool, drilling process, conventional drilling, peck-drilling.

1 Introduction

Nickel-based superalloy is a kind of metal material based on iron, nickel and cobalt element and has excellent high-temperature strength, good oxidation and corrosion resistance, good fatigue and fracture toughness[1]. Thus, nickel-based superalloy is widely employed in the manufacture of high-temperature components of aero jet engines and industrial gas turbines. At present, the application proportion of nickel-based superalloy in advanced aircraft engines has been more than 35%. Furthermore, due to the complex and harsh working environment, it has high machining quality requirement for most nickel-based superalloy parts[2].

The machinability refers to the difficulty of machining mechanical engineering materials. The factors affecting the machinability have mainly mechanical properties, chemical composition, heat treatment state and metallographic structure of machined materials [3]. The machinability is often evaluated by the tool life, cutting force, machining accuracy and surface quality when cutting a certain engineering material [4-5]. According to the difference of machinability, mechanical engineering materials can

be roughly divided into three categories: easy-to-cutting materials, common materials and difficult-to-cutting materials. Nickel-based superalloy is a typical difficult-to-cutting material due to its large high-temperature strength, high work-hardening tendency and low thermal conductivity. When cutting the nickel-based superalloy, the specific cutting force is very large, the cutting temperature is very high and the machining quality is hard to be guaranteed [6-9]. Furthermore, the elements of titanium and nickel in nickel-based superalloy can also accelerate tool wear and tool-edge breakage [10-11].

Drilling is a usual hole-making technology, but it is also a semi-closed cutting process and its performances of chip-breaking and cooling are far less than those of turning and milling. Therefore, the precision drilling of nickel-based superalloy has always been a key technical problem in the field of advanced machining [12]. Imran et al.[13-14] researched the surface integrity of drilling Inconel 718 and found that a metamorphic layer with nanostructure was formed on the machined surface because of the combined action of cutting heat and cutting force, the lubrication condition and cutting parameters were important

influencing factors of the thickness of the metamorphic layer. The study of Chen showed that the tool failure process could be divided into four stages when the TiAlN coated cemented carbide twist drill was used to drilling Inconel 718, which included coating flaking, flank wear, micro breakage and fatigue fracture, high friction force was the primary reason for tool failure [15].

Based on the experiments of drilling Inconel 718, Sharman found that the tool geometry has a significant influence on its service life [16]. Oezkaya et al. [17] developed a novel flank face twist drill and conducted the drilling test of Inconel 718, the results showed that the novel twist drill could achieve a longer tool life. Qin et al. [18] conducted the comparative research of different cooling modes during the drilling of Inconel 718, and the results indicated that the internal spray cooling could achieve more accurate hole diameter, longer tool life and higher surface quality than the external cooling. The research of Jiménez et al. [19] indicated that, compared to conventional drilling of Inconel 718, the peck-drilling

can reduce tool wear and achieve better machining quality. The above research showed that the cutting tool and the drilling process are two important factors that affect the quality and efficiency.

In this paper, based on the tests of conventional drilling of three twist drills with different materials and structures, the drilling machinability of Inconel 718 was evaluated comprehensively by drilling force, tool wear and machining quality, the cutting tools suitable for drilling nickel-based superalloy were chosen. Then the peck-drilling technique was used for improving the machinability of nickel-based superalloys, and the change trends of cutting force, machining accuracy and surface quality during peck-drilling were discussed deeply. Finally, the technological methods for the precision-drilling of nickel-based superalloy were put forward.

2 Experimental conditions

Inconel 718 employed widely in the industry field was chosen as experimental material, its mechanical properties are shown in Table 1.


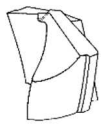

Tab. 1 Mechanical properties of Inconel 718

Tensile strength σ_b (N·mm ⁻²)	1229 ^a , 1019 ^b
Yield strength $\sigma_{0.2}$ (N·mm ⁻²)	1055 ^a , 876 ^b
Extensibility 4D δ (%)	12
Cross-section shrinkage rate Φ (%)	15 ^c
a. Room temperature properties.	
b. High temperature (650 °C) properties.	
c. No fracture for 24 hours when loaded 730N/mm ² at 650 °C	

At present, the tool materials used in machining nickel-based superalloy include high speed steel (HSS), cemented carbide, ceramics and cubic boron nitride (CBN), while HSS and cemented carbide are generally used to manufacture complex cutting tools,

such as small and medium diameter twist drills and end mills [20-21]. In this research, three kinds of commercial twist drills with different materials and structures were selected as test tools and their basic information is listed in Table 2.

Tab. 2 Twist drills used in the experiments

Tool type	General HSS twist drill	HSS-Co twist drill	KDG303 twist drill
Tool materials	W18Cr4V	W2Mo9Cr4VCo8	YK20F carbide
Point angle (°)	140	140	140
Structure of clearance face			
	Single clearance angle	Dual clearance angle	Dual clearance angle
Helix angle (°)	30	30	30
Diameter (mm)	6	6	6
Coating	Uncoated	Uncoated	TiAlN

The workpiece was a round bar with a diameter of 10mm and a length of 45mm. The workpiece was clamped to the top of Kistler 9272 dynamometer by a self-made chucking and the dynamometer was bolted to the workbench of XK714 NC milling machine. During the experiments, the thrust force and torque were obtained by the Kistler 9272 dynamometer. After the

experiments, the Leica KL300 stereomicroscope was used to detect tool wear, the diameter and roundness of the machined hole. Finally, the machined hole was cut open along its axis, and the topography and roughness of the inner surface were measured by the Bruker interferometer. Figure 1 shows the schematic diagram of drilling process and measurements.

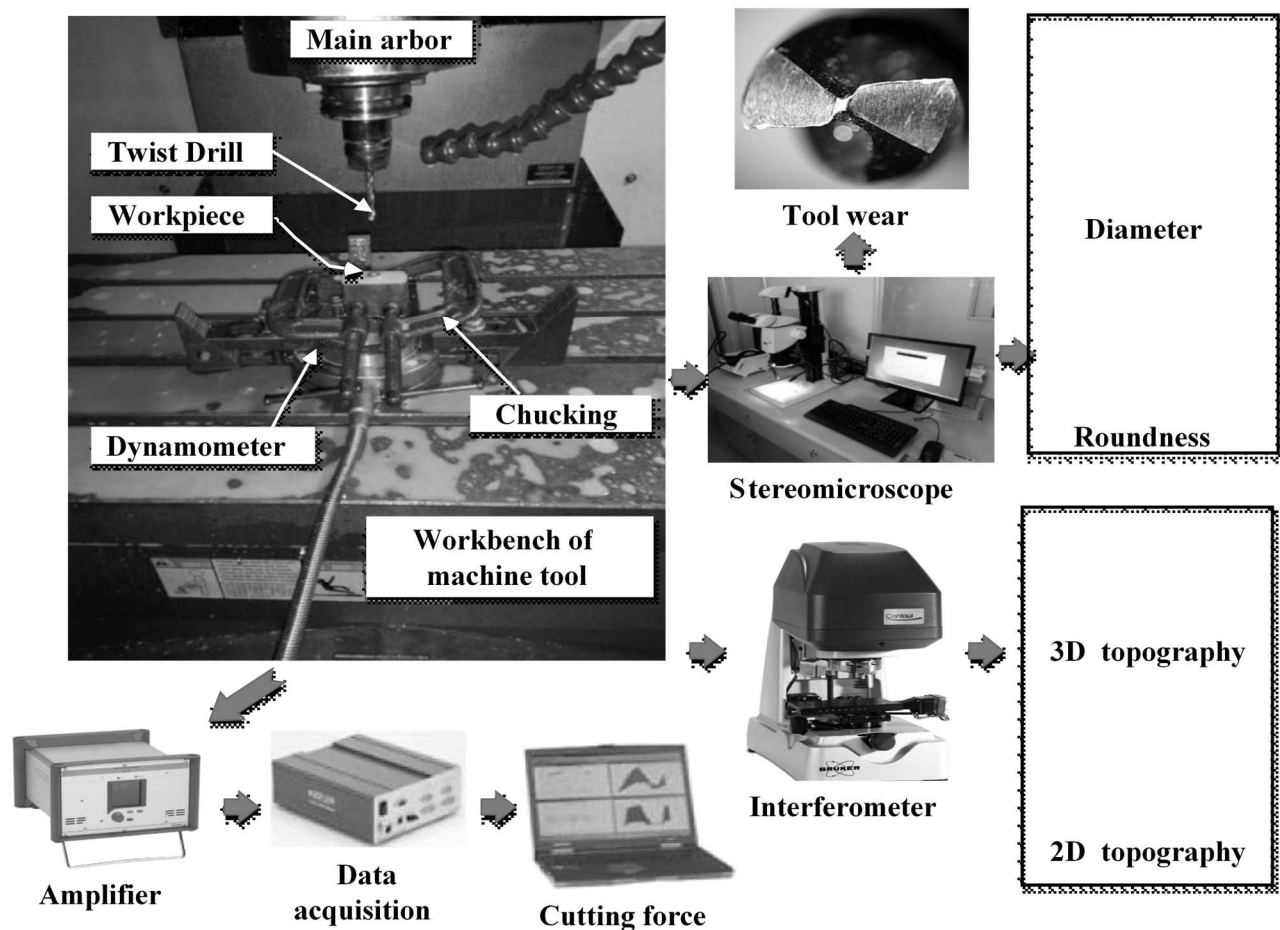


Fig. 1 Schematic diagram of drilling process and measurements

3 Evaluation of drilling machinability of Inconel 718 under different twist drills

3.1 Experimental parameters

The experimental parameters are listed in Table 3. Considering that the cemented carbide has a higher

heat resistance and wear resistance, the spindle speed and feedrate of KDG303 twist drill were as twice as those of HSS twist drills. Three kinds of twist drills were all used to drilling the blind hole with a diameter of 6mm and a depth of 12mm, and the machinability of Inconel 718 was evaluated by drilling force, tool wear and machining quality.

Tab. 3 Experimental parameters

Tool Type	General HSS	HSS-Co	KDG303
Spindle speed n (r/min)	300	300	600
Feedrate f (mm/min)	6	6	12
Feed per rotation f_r (mm/r)	0.02		
Lubrication mode	Flood		

3.2 Difference of drilling force under three twist drills

3.2.1 Thrust force and torque

Figure 2 shows the waveforms of drilling force under different twist drills, which represent the instantaneous change trend of thrust force F_z and torque M_z with the increase of cutting time and drill-in depth. These waveforms were obtained after drilled the same number of holes. The following characteristics can be seen in Figure 2.

- (1) With the increase of cutting time, all waveforms of thrust force showed an obvious upward trend in general. The thrust force fluctuation of the KDG303 twist drill was much smaller than that of general HSS and HSS-Co twist drill.
- (1) All torque waveforms appeared a large initial fluctuation. However, with the increase of cutting time and drill-in depth, the torque fluctuation gradually became smaller.

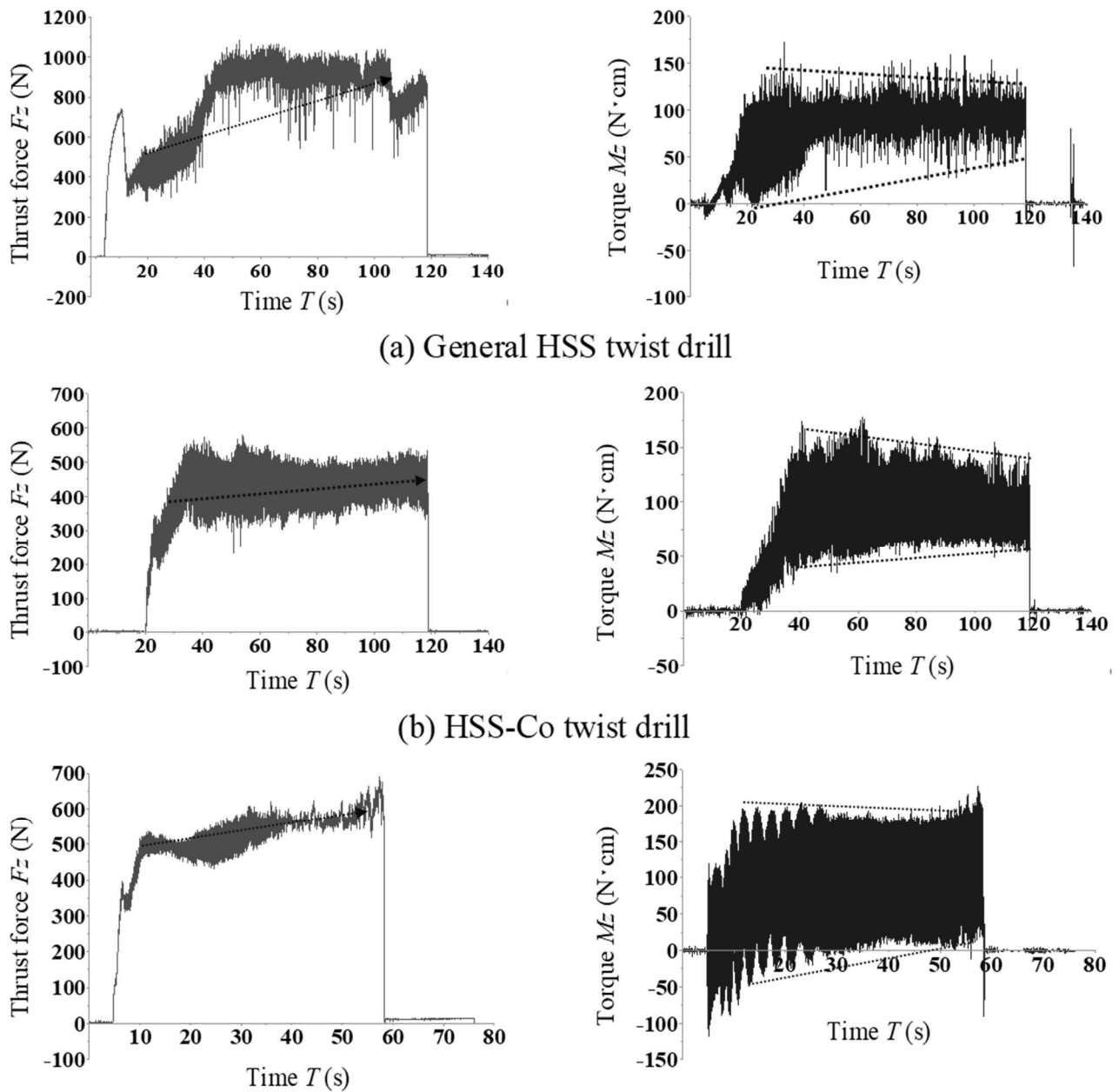


Fig. 2 Waveforms of thrust force and torque under different twist drills

Figure 3 shows the maximum thrust force F_{zmax} and maximum torque M_{zmax} under different twist drills, which were extracted from the waveforms in Figure 2. According to Figure 3, the maximum torques of three twist drills are 177.8, 168.5, and 201.8 N·cm respectively, with little difference. However, the maximum thrust forces are quite different, 1043, 536 and 618.8 N respectively. It is noticed that the feedrate of KDG303 twist drill was twice that of general HSS and HSS-Co twist drills, and its MRR (material removal rate) and machining efficiency were also doubled. Therefore, it can be inferred that, with the same cutting parameters, the minimum drilling force can be achieved by using KDG303 twist drill, followed by the HSS-Co twist drill, while the drilling force of general HSS twist drill is the largest.

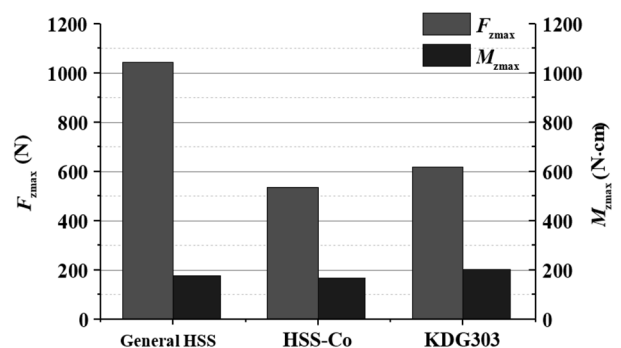


Fig. 3 Maximum thrust force and torque under different twist drills

3.2.2 Reasons for the difference of drilling force

Figure 4 is the decomposition graph of drilling process and drilling force.

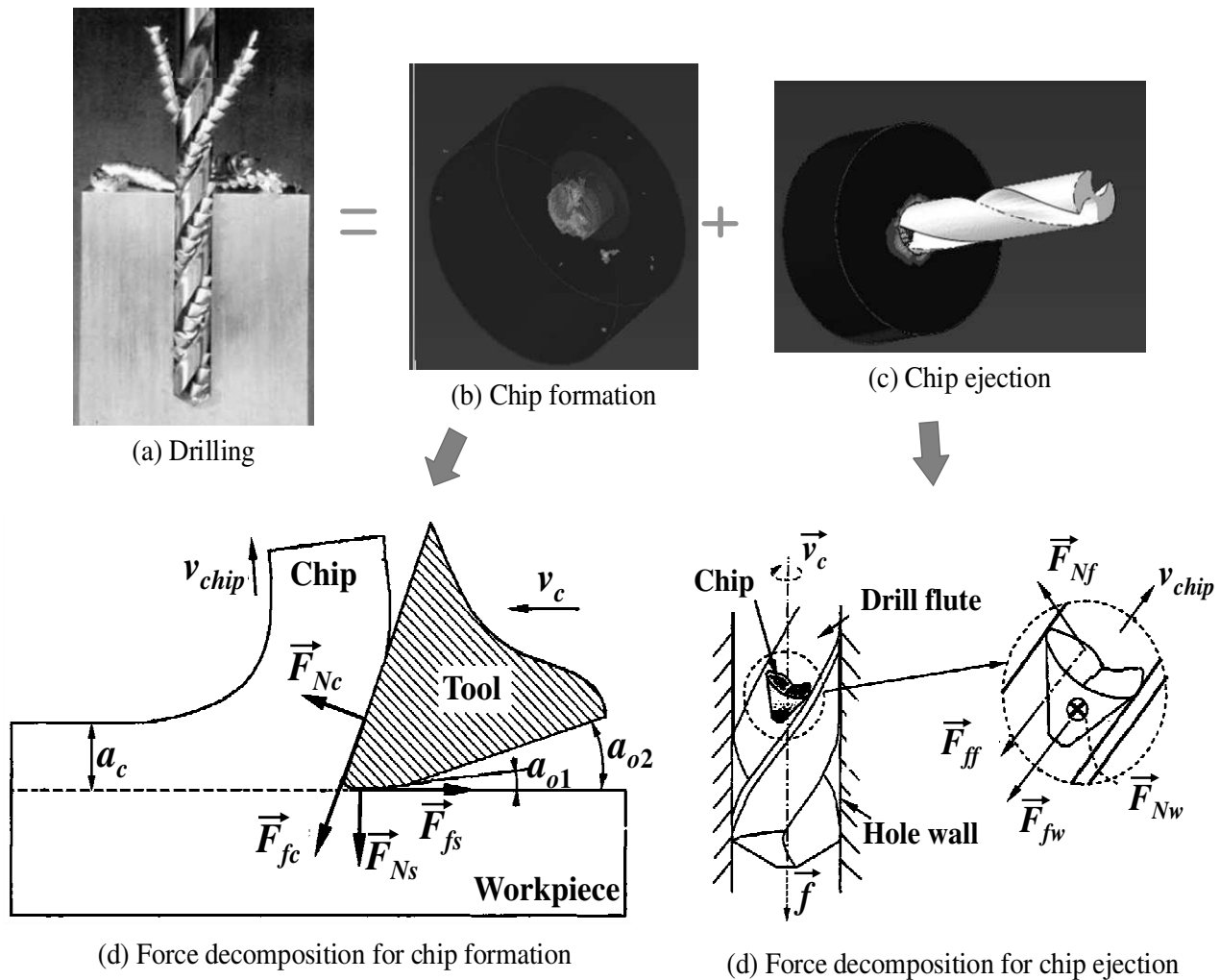


Fig. 4 Decomposition graph of drilling process and drilling force

According to Figure 4(a) 4(b) and 4(c), the drilling process can be considered to be composed of chip formation and chip ejection two stages, therefore the drilling force mainly derived from these two stages. If choosing a tool element and its corresponding chip element as the analysis object, the action forces for chip formation and chip ejection can be shown in Figure 4(d) and 4(e). In the stage of chip formation, the action forces include the friction force \vec{F}_{fc} and the normal force \vec{F}_{Nc} between the tool rake face and the bottom of

the chip, the friction force \vec{F}_{fs} and the normal force \vec{F}_{Ns} between the tool clearance face and the machined surface. In the stage of chip ejection, the action forces include the friction force \vec{F}_{ff} and the normal force \vec{F}_{Nf} between the chip and the drill flute, the friction force \vec{F}_{fw} and the normal force \vec{F}_{Nw} between the chip and the hole wall.

Based on the above decomposition, the resultant force of the analyzed element \vec{F}_{total} can be written as equation (1).

$$\vec{F}_{total} = \vec{F}_{fc} + \vec{F}_{Nc} + \vec{F}_{fs} + \vec{F}_{Ns} + \vec{F}_{ff} + \vec{F}_{Nf} + \vec{F}_{fw} + \vec{F}_{Nw} \quad (1)$$

Therefore, the thrust force F_z and torque M_z can be approximately expressed as equation (2) and (3).

$$\begin{aligned} F_z &= 2 \sum_0^{D/2} (\vec{F}_{total} \cdot \vec{f}) \\ &= 2 \sum_0^{D/2} [(\vec{F}_{fc} + \vec{F}_{Nc} + \vec{F}_{fs} + \vec{F}_{Ns} + \vec{F}_{ff} + \vec{F}_{Nf} + \vec{F}_{fw} + \vec{F}_{Nw}) \cdot \vec{f}] \end{aligned} \quad (2)$$

$$\begin{aligned} M_z &= 2 \sum_0^{D/2} (\vec{F}_{total} \cdot \vec{v}_c \cdot r_e) \\ &= 2 \sum_0^{D/2} [(\vec{F}_{fc} + \vec{F}_{Nc} + \vec{F}_{fs} + \vec{F}_{Ns} + \vec{F}_{ff} + \vec{F}_{Nf} + \vec{F}_{fw} + \vec{F}_{Nw}) \cdot \vec{v}_c \cdot r_e] \end{aligned} \quad (3)$$

Where:

D ...The diameter of the twist drill,

\vec{f} and \vec{v}_c ...Respectively the unit vectors along feedrate direction and cutting speed direction,

r_e ...The action radius of the analysed element.

According to equation (2) and (3), some characteristics of drilling forces showed in Figure 2 can be clarified. In the process of drilling, the drill-in depth and the chip ejection path length will constantly increase with the rise of cutting time, which can cause the obvious increase of friction force \vec{F}_{ff} and \vec{F}_{Nw} , so the thrust force F_z will raise with the increase of cutting time. From Figure 4(d), the second clearance angle α_{o2} can reduce the contact area between the tool clearance face and machined surface and improve the action effect of cutting fluid, which helps to decrease the action force \vec{F}_{fs} and \vec{F}_{Ns} . Therefore, the HSS-Co and KDG303 twist drill with dual clearance angle can achieve smaller thrust force and torque than the general HSS twist drill with single clearance angle.

Furthermore, the drill-in run out of twist drills can bring a larger initial fluctuation of drilling force, while the high stiffness of carbide can reduce the thrust force fluctuation of KDG303 twist drill.

3.3 Wear characteristics of three twist drills

Figure 5 shows the microphotographs of different twist drills. Since three twist drills have different mechanical performances, the microphotograph of general HSS twist drill was acquired after drilled two holes, while the microphotographs of HSS-Co and KDG303 twist drills were acquired after drilled 12 holes. According to Figure 5, the failure characteristics of three twist drills can be described as the following.

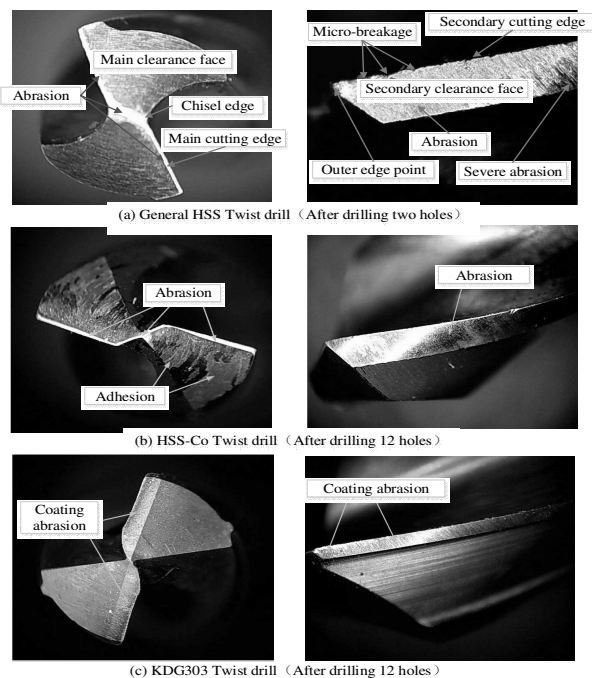


Fig. 5 Microphotographs of different twist drills

- (1) After only two holes were drilled, the chisel edge and the secondary clearance faces of general HSS twist drill have been seriously worn, and the main cutting edges have also taken on a bit of abrasion. At the same time, some micro-breakages have appeared at the secondary cutting edges, and the closer to the outer edge point, the more serious the breakage was.
- (2) The failure mode of HSS-Co twist drill was the same as that of general HSS twist drill, but its wear resistance was much better. Even after machined 12 holes, its wear degree was still less than that of general HSS twist drill. However, it happened serious adhesion on the main clearance faces.
- (3) After machined 12 holes, there was only a small amount of coating abrasion appearing at the main and secondary clearance faces of KDG303 twist drill. Therefore, the KDG303 twist drill showed the best wear resistance.

3.4 Machining accuracy and surface quality of three twist drills

3.4.1 Machining accuracy

Figure 6 shows the machining accuracy with different twist drills. The measured holes were the same as that in Figure 2. The hole expansion size ΔD represents the difference between the actual aperture and the ideal aperture, and the roundness error Re refers to the entrance roundness error of the machined hole. From Figure 6, the hole expansion size ΔD and the roundness error Re have the same variation trend. The machining accuracy of general HSS was the worst, the secondary the HSS-Co, and the highest the KDG303. This result is closely related to the drilling force and wear resistance of three twist drills.

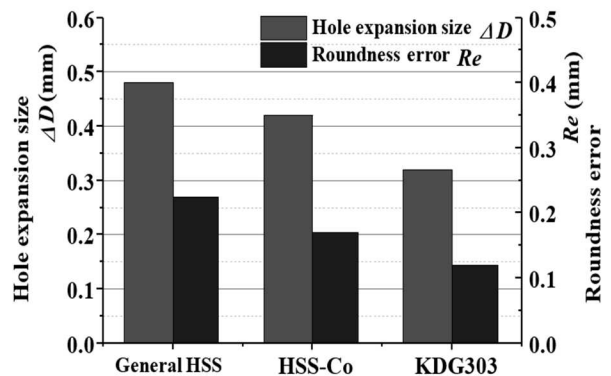
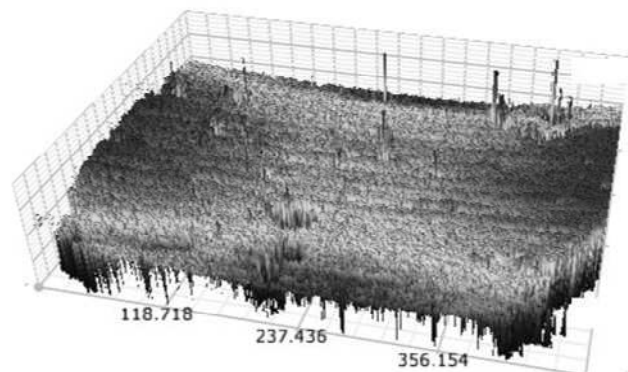
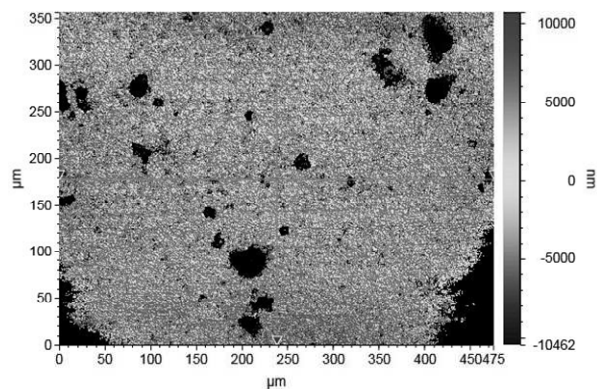


Fig. 6 Machining accuracy with different twist drills

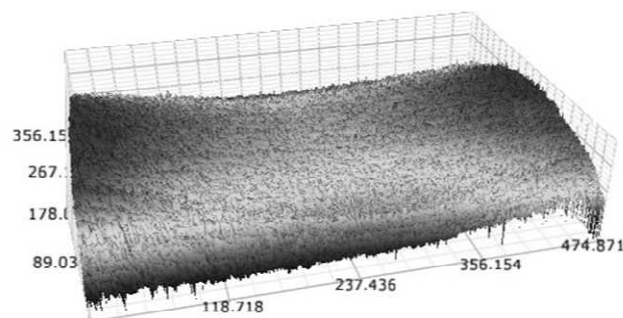
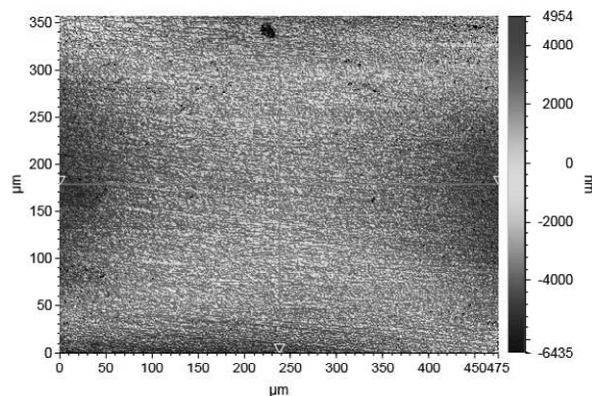
3.4.2 Surface quality

Figure 7 shows the surface topography of machined holes with three twist drills. From Figure 7, the machined surface with the general HSS twist drill appeared many peaks and pits that could be caused by micro-breakages of the secondary cutting edge. The surface topography with the HSS-Co twist drill was most regular and smooth. The machined surface with KDG303 twist drill was relatively smooth, but it has some tool marks and vertical stripes, which should be related to the higher feedrate and larger MRR of KDG303 twist drill.

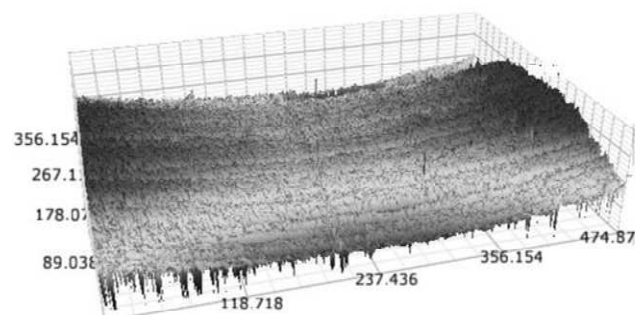
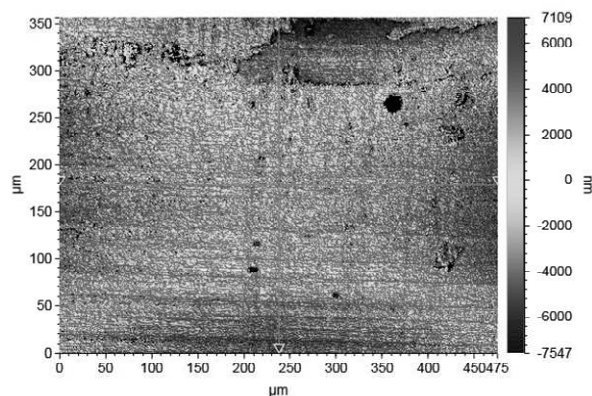
According to the above results, Inconel 718 shows poor machinability under the general HSS twist drill because of larger drilling torque, serious tool wear and poor machining quality. Therefore, this tool is not suitable for drilling nickel-based superalloy. The HSS-Co twist drill has moderate drilling performance and is suitable for the situation of low feedrate. By using the KDG303 twist drill, Inconel 718 shows good machinability, but in order to obtain better surface quality, the smaller feedrate should be considered. Furthermore, the tool structure of dual clearance angle is more beneficial to reduce drilling force and improve machining quality.



(a) General HSS Twist drill



(b) HSS-Co Twist drill



(c) KDG303 Twist drill

Fig. 7 Surface topography of machined holes with three twist drills

4 Machining effect of Inconel 718 under peck-drilling process

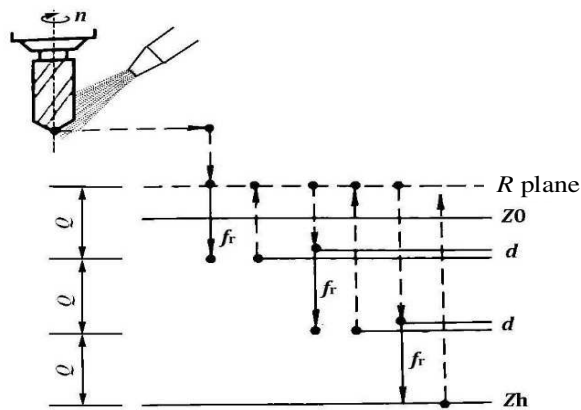


Fig. 8 Illustration of peck-drilling

Tab. 4 Experimental conditions of peck-drilling

Spindle speed n (r/min)	400
Feedrate f (mm/min)	8
Feed per rotation f_r (mm/r)	0.02
Depth of peck Q (mm)	1, 1.5, 2, 2.5, 12
Cutting tool	KDG303 twist drill
Lubrication mode	Flood

The peck-drilling is a step-by-step hole-making technique that transforms continuous cutting into interrupted cutting. It can improve not only the effect of chip breaking and chip ejection but also the cooling and lubrication performance of cutting fluid, hence it is very adaptable to drilling the deep hole and difficult-to-cutting material [22-23]. Figure 8 is the illustration of peck-drilling. In the process of peck-drilling, the

tool drills into a peck depth Q firstly, and withdraws from the cutting area to the R plane that is located at a certain height on the upper surface of the workpiece for an instantaneous stay, then reenters into the hole for next drill-in. The drill tool repeats this movement until the entire hole depth is drilled out.

The peck depth Q is an important parameter of peck-drilling, which has an important influence on tool life, machining quality and machining efficiency [24]. Therefore, the influence of peck depth Q should be deeply analyzed. Table 4 shows the experimental conditions of peck-drilling. Because the depth of the machined hole is 12mm, it represents the situation of conventional continuous drilling when $Q=12$ mm.

4.1 Influence of peck depth Q on drilling force

Figure 9 shows the cutting force waveforms of conventional drilling and peck-drilling. According to Figure 9, the thrust force and torque of peck-drilling decreased periodically to zero due to the periodic withdrawal of the twist drill. Compared with conventional drilling, the thrust force waveform of peck-drilling had little change, but the fluctuation and maximum value of torque were significantly reduced [25-26].

Figure 10 shows the maximum drilling force under different Q . According to Figure 10, compared with conventional drilling ($Q=12$ mm), the peck-drilling reduced the maximum thrust force F_{zmax} by 30~60N, about 5~8%, and the maximum torque M_{zmax} by 70~87N·cm, about 25~40%. The maximum torque did not change significantly with the increase of the peck depth Q , while the maximum thrust force decreased evidently when the peck depth Q was larger.

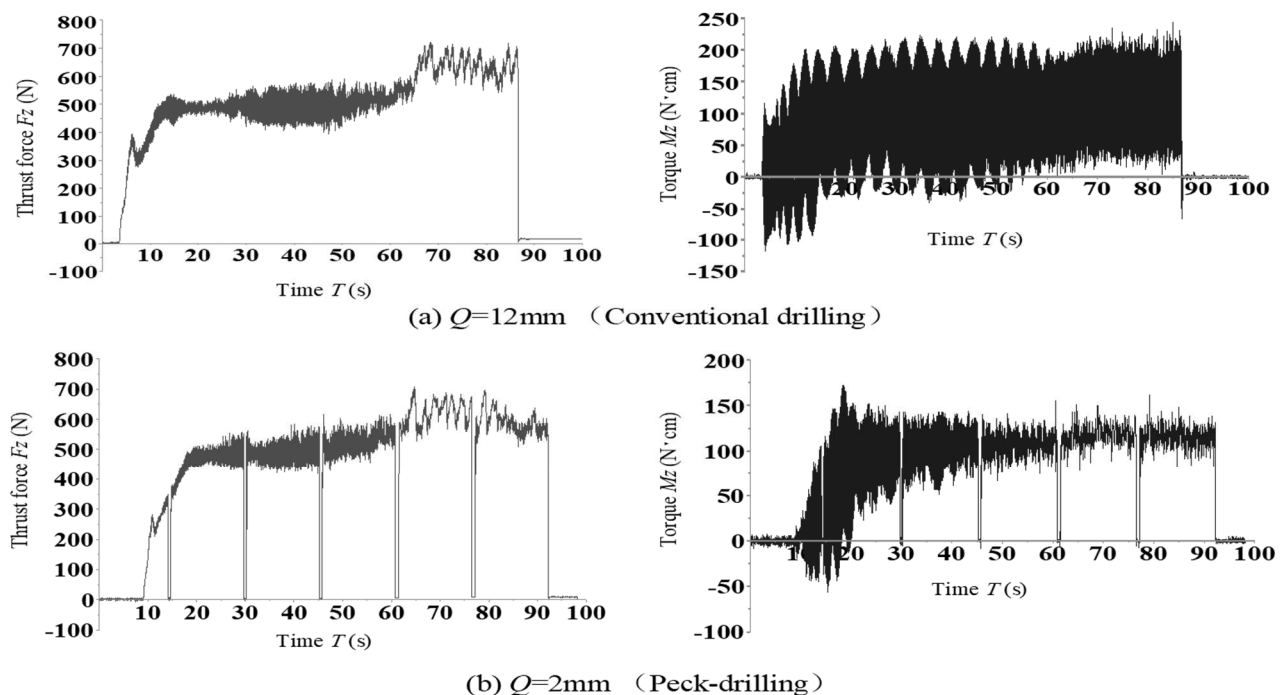


Fig. 9 Cutting force waveforms of conventional drilling and peck-drilling

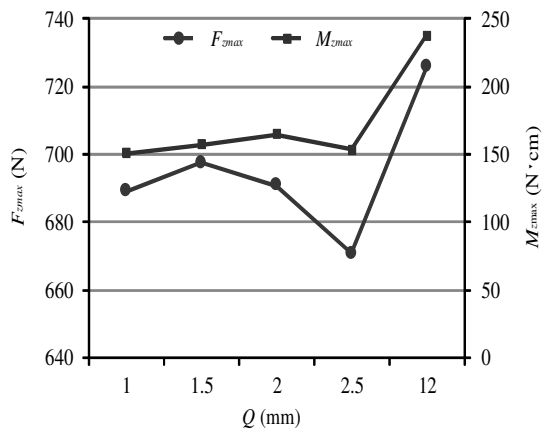


Fig. 10 Maximum drilling force under different Q

Figure 11 shows the peak-peak value of drilling force under different Q . This value is equal to the difference between maximum force and minimum force in the stable cutting stage, and is often used to evaluate the stability of the cutting process. In Figure 11, $F_{zp-p} = F_{zmax} - F_{zmin}$, $M_{zp-p} = M_{zmax} - M_{zmin}$. Compared to conventional drilling, the peck-drilling reduced the peak-peak value of thrust force F_{zp-p} by 20~50N, about 8~20%, and the torque peak-peak value M_{zp-p} by 160~180N·cm, about 67~75%. However, the peak-peak values of thrust force and torque did not change significantly with the rise of the peck depth Q .

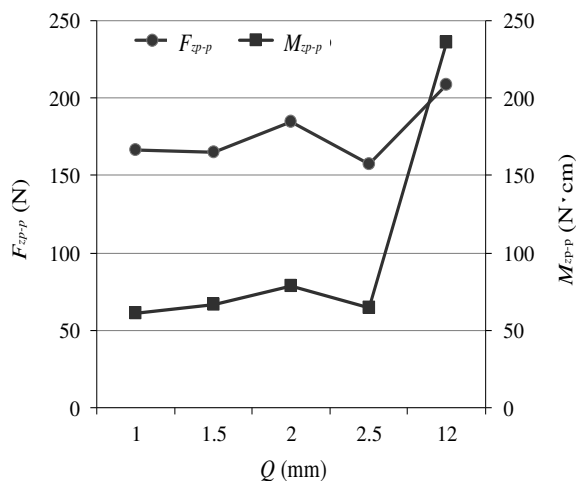


Fig. 11 The peak-peak value of drilling force under different Q

4.2 Influence of peck depth Q on machining accuracy

Figure 12 shows the hole expansion size ΔD and roundness error R_e under different Q , which are usually used to evaluate the dimensional and shape accuracy of machined holes. As shown in Figure 12, the hole expansion size ΔD of peck-drilling was much smaller than that of conventional drilling ($Q=12$ mm)

due to the reduction of drilling force and the improvement of drilling stability, and the minimum was 0.146mm when $Q=2.5$ mm. However, the measurement results of roundness error R_e show that the peck-drilling can't obtain higher shape accuracy than conventional drilling. This result should be caused by the periodic withdrawal and repeated cutting of the twist drill.

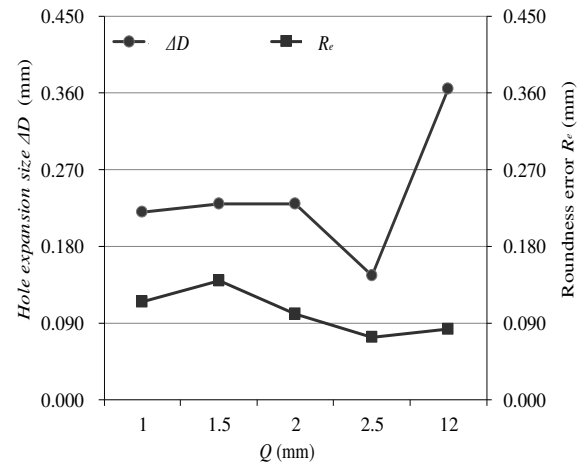
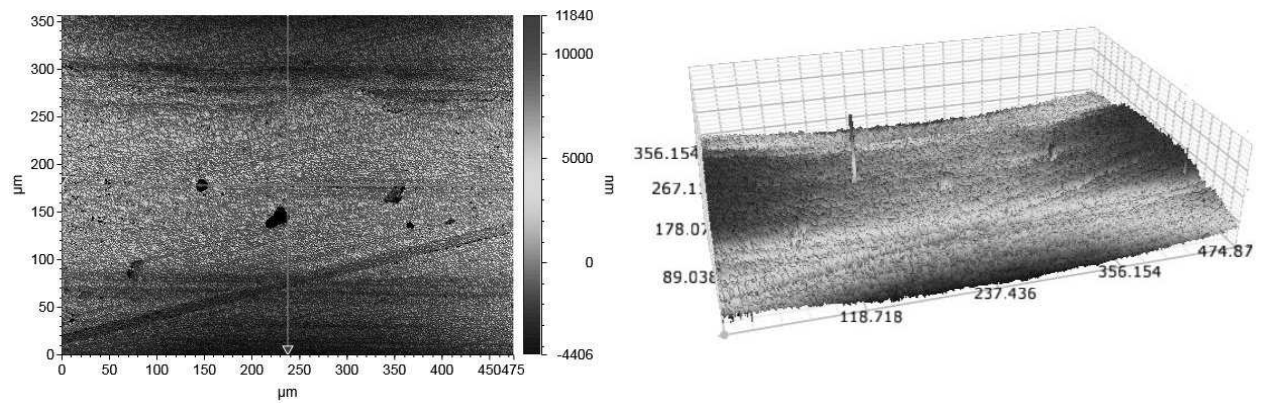
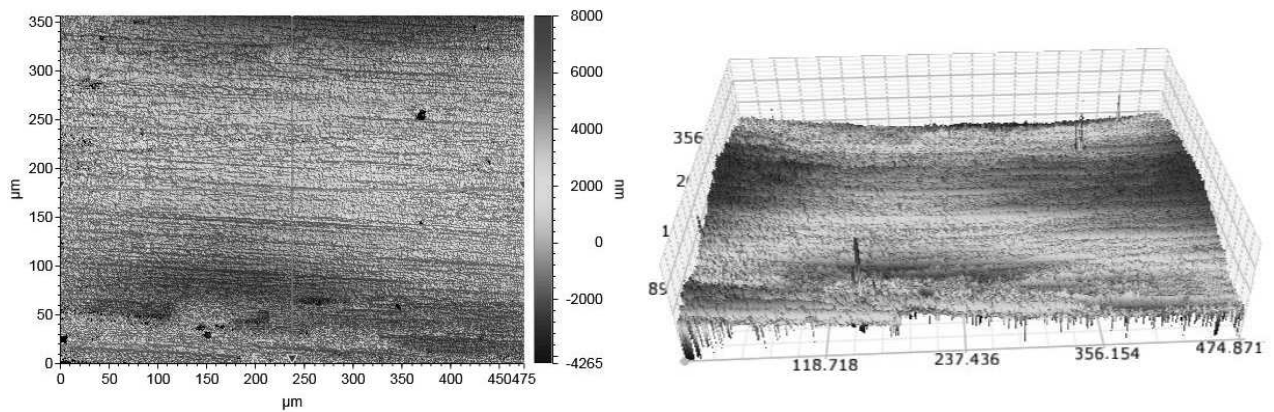
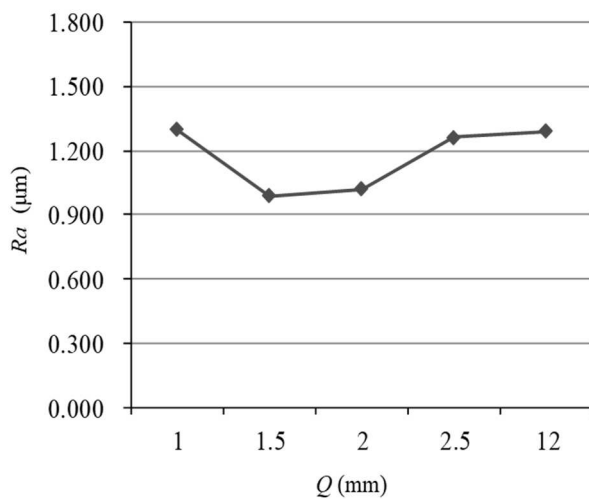


Fig. 12 Hole expansion size and roundness error under different Q

4.3 Influence of Q on surface quality

Figure 13 shows the surface topography of conventional drilling and peck-drilling. According to Figure 13, the surface topography of peck-drilling was more regular and smoother, and there were fewer scratches and bulges on the machined surface. Besides, both Figure 13 (a) and Figure 7 (c) were the machined surface of conventional drilling under KDG303 twist drill, because the feedrate for Figure 13 (a) was relatively smaller, the corresponding machined surface was smoother. Therefore, reducing the feedrate is a feasible method to improve surface quality.

Figure 14 is the surface roughness under different Q . As shown in Figure 14, when the peck depth Q was equal to 1 and 2.5mm, the surface roughness of peck-drilling was approximately equal to that of conventional drilling ($Q=12$ mm). When Q was equal to 1.5 and 2mm, the surface roughness was significantly improved. As to peck-drilling, the rise of Q will increase the chip length, while the longer chip is prone to scratch the machined surface in the process of ejection. On the other hand, if Q is too small, more tiny chips will be generated and squeezed into the gap between the tool clearance face and the machined surface, which also deteriorate the surface quality. Therefore, the appropriate Q is very important for exerting the advantage of peck-drilling and improving the drilling quality of nickel-based superalloy.

(a) $Q=12\text{mm}$ (Conventional drilling)(b) $Q=2\text{mm}$ (Peck-drilling)**Fig. 13** Surface topography of conventional drilling and peck-drilling**Fig. 14** Surface roughness under different Q

5 Conclusion

Based on the experimental research of drilling Inconel 718, some technological methods for improving the drilling machinability of nickel-based superalloy can be put forward.

- (1) The general HSS twist drill can't be used to drilling nickel-based superalloy because of poor wear resistance, while the HSS-Co twist

drill is suitable for the situation of low feedrate. The KDG303 twist drill has good wear resistance and high machining quality, which can meet the needs of drilling nickel-based superalloy.

- (2) The tool structure of dual clearance angle is more beneficial to reducing the drilling force and improving the lubrication conditions, which helps to decrease tool wear and improve machining quality. Therefore, the structure optimization of the clearance surface is an effective method to realize the precision drilling of nickel-based superalloy.
- (3) In contrast to conventional drilling, the peck-drilling can not only reduce the drilling force but also improve machining accuracy and surface quality. Especially, it has significant advantages in reducing maximum torque, torque fluctuation and dimensional accuracy. The maximum and peak-peak value of drilling torque can be reduced by 25~40% and 67~75% respectively, and the hole

diameter error can be halved. Therefore, the peck-drilling can not only solve the problem of drilling deep holes, but also can meet the needs of drilling difficult-to-cutting materials.

- (4) The appropriate peck depth Q is very important for exerting the advantage of peck-drilling. In this research, when the peck depth Q is about 2 mm, the best process effect can be obtained.

Acknowledgement

This research was financially supported by the National Natural Science Foundation of China, Grant Number 52175397, the Henan Province Science and Technology Research Projects, China, Grant Number 212102210355, the Key Scientific Research Project in Universities of Henan Province, China, Grant Number 21A460015 and 22A460019.

References

- [1] ZICKLER, G.A., SCHNITZER, R., RADIS, R., HOCHFELLNER, R., SCHWEINS, R., STOCKINGER, M., LEITNER, H. (2009). Microstructure and Mechanical Properties of the Superalloy ATI Allvac® 718Plus™. *Materials Science and Engineering: A*, 523(1-2): 295-303. Doi:10.1016/j.msea.2009.06.014
- [2] YIN, Q., LIU, Z., WANG, B., SONG, Q., & CAI, Y. (2020). Recent Progress of Machinability and Surface Integrity for Mechanical Machining Inconel 718: A Review. *The International Journal of Advanced Manufacturing Technology*, 109: 215-245. Doi:10.1007/s00170-020-05665-4
- [3] SINHA, M. K., PAL, A., KISHORE, K., SINGH, A., SANSANWAL, H., & SHARMA, P. (2022). Applications of Sustainable Techniques in Machinability Improvement of Superalloys: A Comprehensive Review. *International Journal on Interactive Design and Manufacturing (IJIDeM)*, 1-26. <https://doi.org/10.1007/s12008-022-01053-2>
- [4] PERVAIZ, S., KANNAN, S., ANWAR, S., & HUO, D. (2022). Machinability Analysis of Dry and Liquid Nitrogen-Based Cryogenic Cutting of Inconel 718: Experimental and FE Analysis. *The International Journal of Advanced Manufacturing Technology*, 118: 3801-3818. <https://doi.org/10.1007/s00170-021-08173-1>
- [5] ÇAKIROĞLU, R. (2021). Machinability Analysis of Inconel 718 Superalloy with AlTiN-Coated Carbide Tool Under Different Cutting Environments. *Arabian Journal for Science and Engineering*, 46: 8055-8073. <https://doi.org/10.1007/s13369-021-05626-3>
- [6] WANG, R., DONG, X., WANG, K., SUN, X., FAN, Z., & DUAN, W. (2019). Two-Step Approach to Improving the Quality of Laser Micro-Hole Drilling on Thermal Barrier Coated Nickel Base Alloys. *Optics and Lasers in Engineering*, 121: 406-415. Doi:10.1016/j.optlaseng.2019.05.002
- [7] JANGALI, S. G., GAITONDE, V. N., KULKARNI, V. N., & MADHUSUDHANA, H. K. (2022). Analyzing the Effect of Cutting Parameters on Forces and Tool-Tip Temperature in Turning of Nickel-Based Superalloy Using FE Simulation. *Materials Today: Proceedings*, 49(Part 5): 1833-1843. Doi:10.1016/j.matpr.2021.08.054
- [8] ZĘBALA, W., STRUZIKIEWICZ, G., & RUMIAN, K. (2021). Cutting Forces and Tool Wear Investigation during Turning of Sintered Nickel-Cobalt Alloy with CBN Tools. *Materials*, 14(7): 1623. Doi:10.3390/ma14071623
- [9] PARIDA, A. K., & MAITY, K. (2021). Study of Machinability in Heat-Assisted Machining of Nickel-Base Alloy. *Measurement*, 170: 108682. Doi:10.1016/j.measurement.2020.108682
- [10] YU, W., MING, W., AN, Q., & CHEN, M. (2021). Cutting Performance and Wear Mechanism of Honeycomb Ceramic Tools in Interrupted Cutting of Nickel-Based Superalloys. *Ceramics International*, 47(13): 18075-18083. Doi:10.1016/j.ceramint.2021.03.123
- [11] KONG, X., YANG, L., ZHANG, H., ZHOU, K., & WANG, Y. (2015). Cutting Performance and Coated Tool Wear Mechanisms in Laser-Assisted Milling K24 Nickel-Based Superalloy. *The International Journal of Advanced Manufacturing Technology*, 77: 2151-2163. Doi:10.1007/s00170-014-6606-9
- [12] ZHOU, Y., LI, H., MA, L., CHEN, J., TAN, Y., & YIN, G. (2020). Study on Hole Quality and Surface Quality of Micro-Drilling Nickel-Based Single-Crystal Superalloy. *Journal of the Brazilian Society of Mechanical Sciences and Engineering*, 42: 341. Doi:10.1007/s40430-020-02427-x
- [13] IMRAN, M., MATIVENGA, P. T., GHOLINIA, A., & WITHERS, P. J. (2011). Evaluation of Surface Integrity in Micro Drilling Process for Nickel-Based Superalloy. *The International Journal of Advanced Manufacturing*

- Technology, 55: 465–476. Doi:10.1007/s00170-010-3062-z
- [14] IMRAN, M., MATIVENGA, P. T., GHOLINIA, A., & WITHERS, P. J. (2014). Comparison of Tool Wear Mechanisms and Surface Integrity for Dry and Wet Micro-Drilling of Nickel-Base Superalloys. *International Journal of Machine Tools and Manufacture*, 76: 49–60. Doi:10.1016/j.ijmachtools.2013.10.002
- [15] CHEN, Y. C., & LIAO, Y. S. (2003). Study on Wear Mechanisms in Drilling of Inconel 718 Superalloy. *Journal of Materials Processing Technology*, 140(1-3): 269–273. Doi:10.1016/S0924-0136(03)00792-1
- [16] SHARMAN, A. R. C., AMARASINGHE, A., & RIDGWAY, K. (2008). Tool Life and Surface Integrity Aspects When Drilling and Hole Making in Inconel 718. *Journal of Materials Processing Technology*, 200(1-3): 424–432. Doi:10.1016/j.jmatprotec.2007.08.080
- [17] OEZKAYA, E., BÜCKER, M., STRODICK, S., & BIERMANN, D. (2019). Thermomechanical Analysis Leading to a Novel Flank Face Design Providing Longer Tool Lives for Tools Used in the Drilling of Inconel 718. *The International Journal of Advanced Manufacturing Technology*, 102: 2977–2992. Doi:10.1007/s00170-019-03417-7
- [18] QIN, X., LIU, W., LI, S., TONG, W., JI, X., MENG, F., LIU, J.H., ZHAO, E. (2019). A Comparative Study between Internal Spray Cooling and Conventional External Cooling in Drilling of Inconel 718. *The International Journal of Advanced Manufacturing Technology*, 104: 4581–4592. Doi:10.1007/s00170-019-04330-9
- [19] JIMÉNEZ, A., ARIZMENDI, M., & SÁNCHEZ, J. M. (2021). Extraction of Tool Wear Indicators in Peck-Drilling of Inconel 718. *The International Journal of Advanced Manufacturing Technology*, 114: 2711–2720. Doi:10.1007/s00170-021-07058-7
- [20] PERVAIZ, S., RASHID, A., DEIAB, I., & NICOLESCU, M. (2014). Influence of Tool Materials on Machinability of Titanium- and Nickel-Based Alloys: A Review. *Materials and Manufacturing Processes*, 29(3): 219–252. Doi:10.1080/10426914.2014.880460
- [21] PANG, K., & WANG, D. (2020). Study on the Performances of the Drilling Process of Nickel-Based Superalloy Inconel 718 with Differently Micro-Textured Drilling Tools. *International Journal of Mechanical Sciences*, 180: 105658. Doi:10.1016/j.ijmecsci.2020.105658
- [22] KHAN, S. A., NAZIR, A., MUGHAL, M. P., SALEEM, M. Q., HUSSAIN, A., & GHULAM, Z. (2017). Deep Hole Drilling of AISI 1045 via High-Speed Steel Twist Drills: Evaluation of Tool Wear and Hole Quality. *The International Journal of Advanced Manufacturing Technology*, 93: 1115–1125. Doi:10.1007/s00170-017-0587-4
- [23] HU, F., XIE, L., XIANG, J., UMER, U., & NAN, X. (2018). Finite Element Modelling Study on Small-Hole Peck Drilling of SiCp/Al Composites. *The International Journal of Advanced Manufacturing Technology*, 96: 3719–3728. Doi: 10.1007/s00170-018-1730-6
- [24] ELTAGGAZ, A., & DEIAB, I. (2019). Comparison of between Direct and Peck Drilling for Large Aspect Ratio in Ti-6Al-4V Alloy. *The International Journal of Advanced Manufacturing Technology*, 102: 2797–2805. Doi: 10.1007/s00170-019-03314-z
- [25] PELLEGRINI, G., & RAVASIO, C. (2022). Experimental Investigation on the Effects of the Geometry of Micro Hole on the EDM Drilling Process. *Manufacturing Technology*, 22(4), 455-460. DOI: 10.21062/mft.2022.053
- [26] KOLLOVÁ, A., & PAUEROVÁ, K. (2022). Superalloys—Characterization, Usage and Recycling. *Manufacturing Technology*, 22(5), 550-557. DOI: 10.21062/mft.2022.070